

***In Silico* Discovery of Complex Molecular Containers**

Dominique Barth, Olivier R.P. David, Franck Quessette, Yann Strozecki, Sandrine Vial*

DAVID UMR 8144, Institut Lavoisier UMR 8180, Université de Versailles St Quentin-en-Yvelines, 45
avenue des Etats-Unis, 78035 Versailles.

Corresponding author: olivier.david@uvsq.fr

Abstract: In the accompanying paper we have introduced *chemglyphs* as symbols for the representation of molecular structures as varied as cryptands, capsules, dendrimers, interlocked systems or 3D periodic frameworks. In the present article, we want to illustrate their utility as tools in chemo-informatics, specifically as an aid in the design of innovative cage-like structures.

Following the pioneering work of Nobel-prize winning supramolecular chemists D.J Cram, J.-M. Lehn and C.J. Pedersen, recent years have experienced spectacular growth of interest for molecular architectures possessing a defined inner-space, and in parallel functional molecular objects were designed and studied, culminating in a second Nobel prize in the field with Jean-Pierre Sauvage, Sir J. Fraser Stoddart and Bernard L. Feringa. Moreover, discrete molecular compounds, in parallel to materials like zeolites or Metal-Organic Frameworks, have been created and used in manifold applications. The sole synthesis of these very complex molecules is a research interest in its own right, usually relying on dynamic assembly of small reactive modules.^{1,2} A first set of applications uses these defined cage-compounds in host-guest chemistry for molecular encapsulation;³ the absorption of gases in particular being a very recent and active field of study,^{4,5} encompassing two facets in supramolecular chemistry: artificial receptors and intrinsic porous materials. More advanced applications not only use such architectures as mere molecular containers but as artificial enzymes, or mimics of them, by studying chemical reactions within their inner space⁶ and more widely with the use of cage-compounds for specific functions.⁷

These molecular flasks were sometimes discovered by accident, but as chemists gained experience, they more and more largely relied on *rational design*.^{8,9,10} With such a concept one usually means a top-down, or deconstructive, approach; that is, having a specific target molecular structure in mind and conceiving accordingly the constitutive modules. The design part thus consists of cutting the targeted architecture into pieces, and selecting the appropriate reactive fragments possessing the connective and geometric properties fitting the planned assembly. This approach proved successful in a number of cases but is inherently limited to the macromolecular assemblies a human brain is prone to imagine. As a result, all experimentally prepared cage compounds are chemical materializations of the canonical regular solids.

The present work exposes a complementary, bottom-up approach, with the enumeration of the feasible cages starting from a given set of modules. Importantly this process of combining *chemglyphs* together does not consider the shape of each module in term of inter-atomic distances and angles, and therefore potentially allows access to virtually all possible cages. As for any enumeration, when human brain is supplemented by a computer, two problems have to be addressed. First, the combinatorial explosion of the number of solutions (*ie* the number of possible cages) while increasing the number of modules available for the construction; and the second one,

related to this explosion, the necessity to have a high-performance screening tool in order to pick out only a few candidates among the overwhelming choice of structures generated.

The research project presented here unfolded in four steps. Step one was the conception of an algorithm for the smart generation of cages libraries using determined sets of *chemglyphs* as entries. Step two saw the selection of a small array of topological criteria for the above mentioned screening purposes. These two first steps required extensive algorithm optimization work to reduce all calculation times, in order to construct cage libraries as large as possible. This resulted in an online application called *kekule-kagome* at <http://kekule.prism.uvsq.fr/> to implement the generation and calculation of relevant indices on any combination of desired *chemglyphs*. With several libraries generated, we then embarked in step three with the validation of the selected criteria by comparing virtual structures having the most highly rated indices with real, experimentally observed, molecular containers. Finally in step four, we explored these libraries in order to single out some fancy and previously unimagined architectures.

Main Section

Generation of cage libraries. The core element of the present work is an algorithm able to generate cage structures from selected *chemglyphs*. The collection of the generated cages then constitutes a library which serves as the raw material for the following steps. The constitution of a library is based on the following principles: first, the user selects the types of *chemglyphs* to be assembled; the connecting pattern for each of them is also defined, subsequently defining the mutually reactive end-groups, the convention being that reactive end group **a** is able to form a link only with **-a**, **b** with **-b** and so on.

The algorithm then starts by concatenating *chemglyphs* together to form trees, in a second step the generated trees are folded by matching the still unpaired connections. Only the saturated structures are finally stored, that is cages in which all connections are paired. The main weakness of this approach is that we may generate cages several times. Hence we detect isomorphic cages all along the process of generation and store only distinct cages in the library. This process is progressively applied to an increasing total number of *chemglyphs* within a structure, hence generating increasing numbers of cage candidates. To make the generation process faster we used two methods. First we have replaced the trees of the first step by paths or cycles, which greatly reduced the number of redundant cages and dramatically improved the generation time. The drawback is that we may miss some cages, but we can prove that for some sets of *chemglyphs* the generation is exhaustive and for others experimentation shows that only cages with bad indices are missed. Secondly, we have improved our first step so that it generates only trees, paths or cycles which can be completely saturated in the second step. In Tables 1 and 2, we give the time to generate all unique maps and calculate their indices for several sets of motifs. The computation has been done on a regular 2015 desktop on a single processor. The code and the exhaustive results of our approach can be found at the following address <http://kekule.prism.uvsq.fr>. The details of the implementation of our generation algorithms are presented in the supplementary material section.

In figure 1 two examples are displayed to illustrate the combinatorial explosion, resulting in intractable calculation times for the high families of $J_n V_n V_n$ and $Y_n I_{3n/2}$ libraries using trees algorithms.

The gain brought by the use of paths and then cycles algorithms is also shown, thus allowing for generation of larger structures in reasonable times.

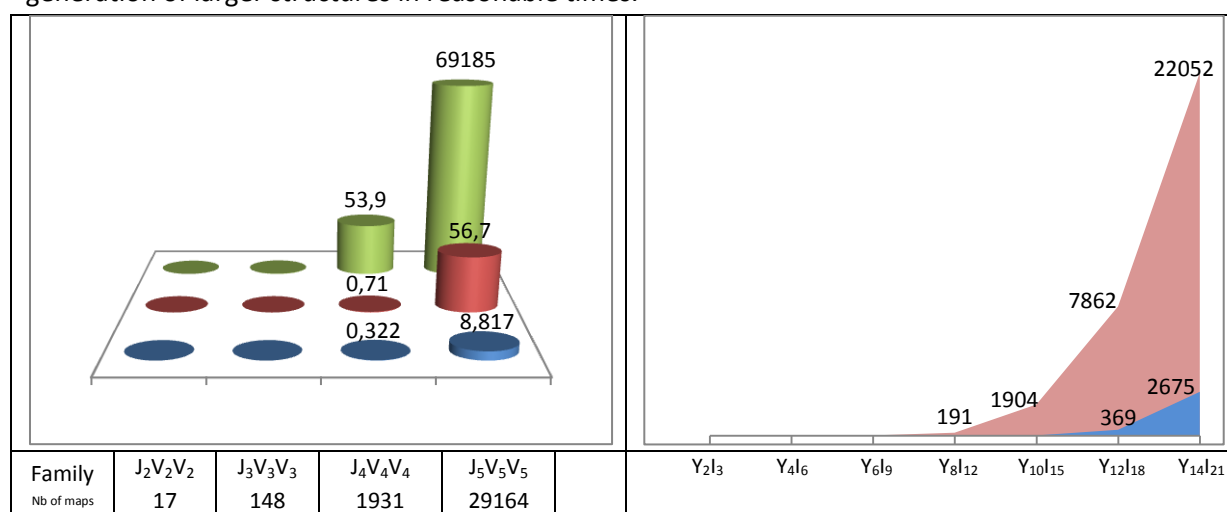


Figure 1. Calculation times according to the family of structures generated. Left: Time (in second) for the generation of JVV libraries, employing tree-based algorithm (in green), path-based (in red) and cycle-based (in blue). Right: Time (in second) for the generation of JVV libraries, employing path-based (in red) and cycle-based algorithms (in blue).

There is still room for improvement in our algorithms, and we recently improved our performances by a factor of two to ten depending on the motifs. However, the number of generated cages is exponential in the number of *chemglyphs* used to assemble them; therefore exhaustive generation will not go much further than what we have achieved. For instance, it is certainly possible to get the maps up to J₆V₆V₆ or J₇V₇V₇ but for larger size we will generate more than a billion of such maps, which are even not easy to store.

The generated library is the collection of each single structure, classified by family, and stored as .cdx files that are readable by ChemDraw®. In this way, the representation can be directly obtained as planar drawings or as 3D views. Figure 2 shows a rendering for the first four families, from X₁I₂ to X₄I₈.

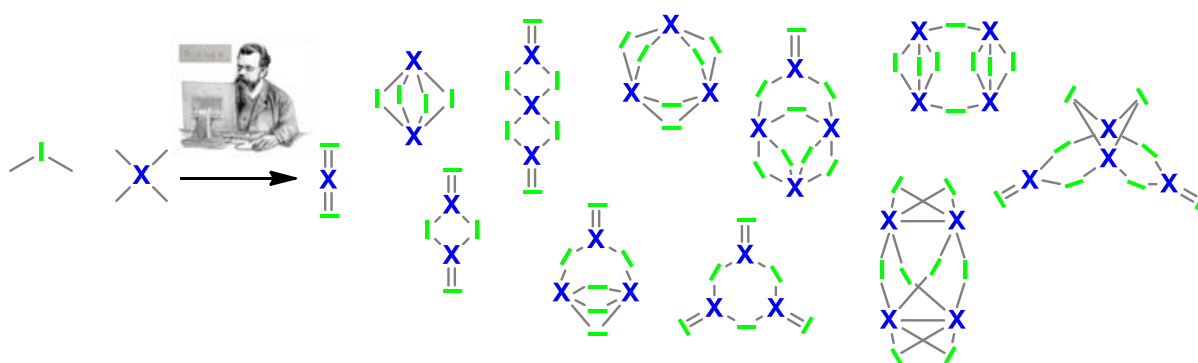


Figure 2. Generation of graphs from chemglyphs X and I (X_nI_{2n}).

From this example, one rapidly realizes that a lot of the generated structures would not be actually described as cages, with flat or linear patterns. Moreover, most of them possess 'double bonds' as two *chemglyphs* can be doubly linked together, an arrangement clearly detrimental for the construction of containers. In step two, we therefore focused on the definition of a small number of

criteria that would numerically capture the relevant parameters for selecting structures fitting what a chemist would call a 'nice cage.'

Classifying libraries – A molecular container has a structure that defines an inner-space partially separated from the outer-space by its atomic constituents. Linear and flat molecules are obviously useless in this context, while good candidates are globular and devoid of unproductive adventitious branches. Two main characteristics can be outlined, that could help defining a proper container. First, it must be somewhat spherical in shape; and then it must be resistant to deformations and cuts. These requirements translate into numerical parameters, defined in graph theory, by two criteria as follows.

Sphericity - In order to be spherical a graph must be *planar*, that is, to cover a sphere without passing-through connections, therefore our generation algorithm was conceived to generate only planar graphs. Moreover, sphericity is related to the symmetry of a graph, and this is numerically evaluated by the number of equivalence classes. Two glyphs are in the same equivalence class if there exists an automorphism (*ie* a symmetry element) that would send one to the other. The fewer the number of different equivalence classes (EC), the more symmetrical the graph, and the more spherical the container.

Resistance – The sturdiness of a cage is linked to the repartition of connections within the architecture, assuring good resistance to deformations and cuts, and this can be estimated by computing the *cut index*. We define the cut index (I_c) as the minimal number of links to cleave in order to cut a graph into two halves, divided by the size of the smallest part. In graph theory, such a partition is called a *sparsest-cut*¹¹. It hence locates the weakest point in the architecture. The best cage candidates must have the highest values of cut index (I_c), showing that their weakest points are still strongly resistant.

Validation of the Indices – To test the relevance of the chosen parameters, we sorted the generated libraries using respectively the number of equivalence classes, and the cut index.

We will examine this screening step with XI structures. In the library of X_nI_{2n} cages, each family contains a single candidate for which the X and I glyphs belong to a unique equivalence class, meaning that all X modules are equivalent, and all I modules are equivalent as well. An exception is found in the X_6I_{12} family for which two candidates are equally placed. In table 1, the structures from X_3I_6 to X_8I_{16} are reproduced. Without any problem, the most symmetrical candidates are picked-up by sorting of the structures with the minimal number of equivalence classes (EC). These ring-shaped architectures actually exist in real chemistry and are materialized by the different classes of cucurbiturils,¹² the X modules being the glycouril moieties and the I modules, the methylene bridges.



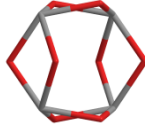
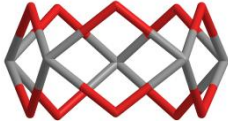
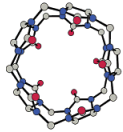

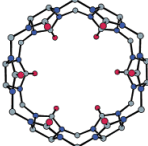
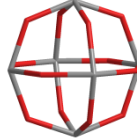

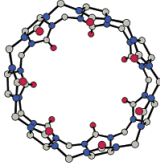

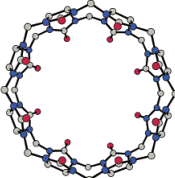
Family	Sphericity best Candidates	Real-life equivalent	Equal firsts
$X_{3 6}$			
$X_{4 8}$			
$X_{5 10}$			
$X_{6 12}$			
$X_{7 14}$			
$X_{8 16}$			

Table 1. For each family of $X_n|_{2n}$ maps, the structure possessing the highest *sphericity* i.e. the minimal number of equivalence classes is displayed, in two instances with some equal firsts; illustration with real cucurbituril compounds.

Among these structures, actually only one is truly container-like, the edge defined octahedron on the fourth line $X_{6|12}$, showing that the sole criterion of perfect symmetry is not discriminating and that a second parameter is therefore mandatory.

This will be the role of the cut index (I_c). Eventually, the most efficient screening process is to rank the candidates, first by I_c values, and then, among the candidates with identical I_c , seeking for the most symmetrical ones, with the fewest number of equivalence classes. In this way, one can pick out the somewhat less symmetrical cages but with great resistance. If the same library is now screened according to the I_c values of its members, the best candidates within each family are different and are displayed in table 2; note that the $X_{4|8}$ and $X_{5|10}$ families possess equally placed structures.

Family	Candidates with the highest I_c	Real-life equivalent	Equal firsts
X_2I_4			
X_3I_6			
X_4I_8			
X_5I_{10}			
X_6I_{12}			
X_7I_{14}			
X_8I_{16}			

Table 2. The best candidates from the same family of X_nI_{2n} maps, with the highest I_c values.

A first observation is that the I_c value properly selects cage-like structures, even if they are slightly less symmetrical. The sturdiness of the graph can be compared with the topological stability of the corresponding molecular cages, though such comparisons must be employed with extreme caution. But in fact, out of these ten candidates, four of them have been experimentally observed and isolated by Pr. Warmuth.¹³ Starting from a tetra-aldehyde cavitand, represented by an X, and ethylenediamine linkers, symbolized by an I. Four different containers X_2I_4 - X_4I_8 - X_6I_{12} - X_8I_{16} could be selectively prepared depending on the solvent employed; emphasizing that under thermodynamic control such assemblies form preferentially.

If we now turn our attention towards another library, what can the panning of Y and I alluvium bring to light? By combining I_c and equivalence classes filters, one can identify in a flash uniform polyhedra based on vertices of degree three within the $Y_n I_{3n/2}$ families: tetrahedron, cube, trigonal, pentagonal and hexagonal prism, as well as the truncated tetrahedron, see figure 2.

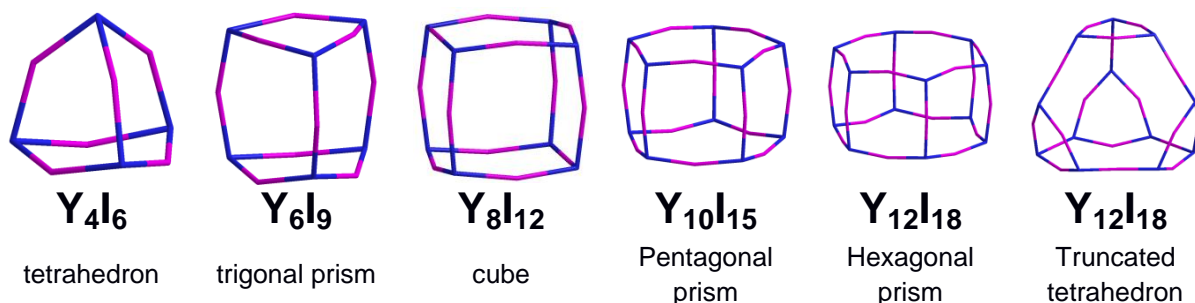
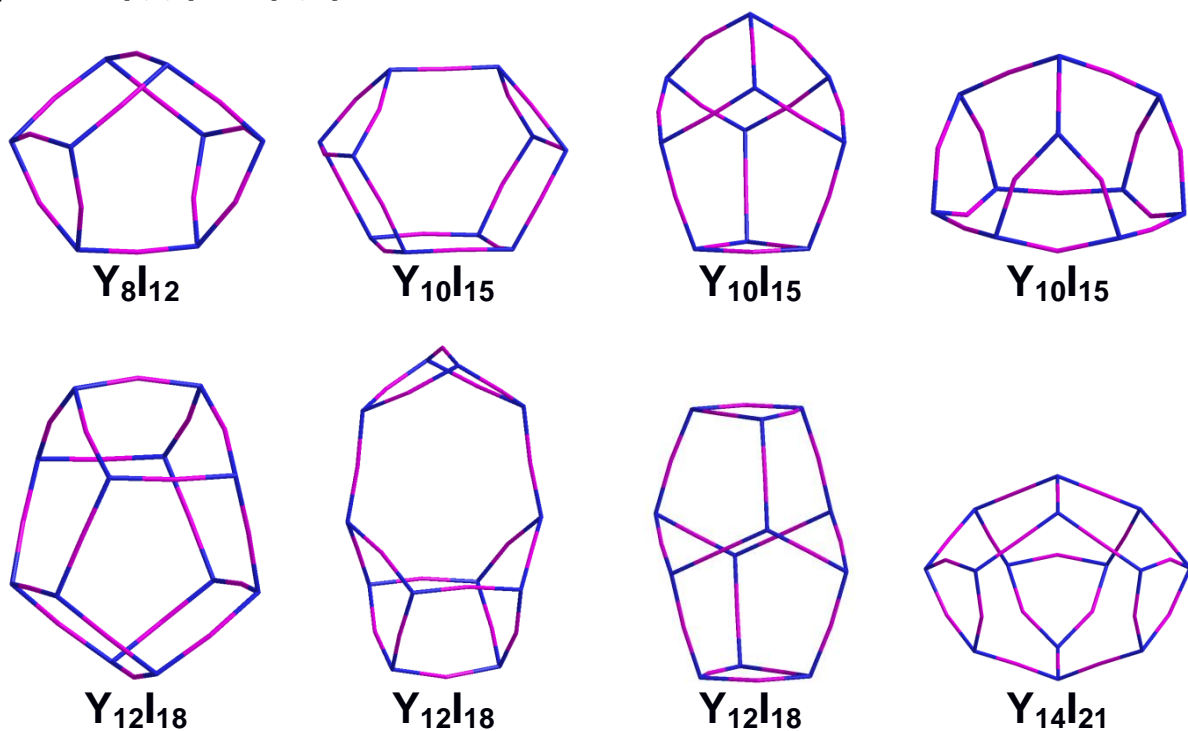


Figure 3. Best candidates with the highest I_c values and maximal sphericity within the $Y_n I_{3/2n}$ families.

To give an ideal of the importance of this filtering process, note that hexagonal prism and the truncated tetrahedron were identified among 369 structures in the $Y_{12} I_{18}$ family, preventing a tedious manual examination of every single architecture.

Discovering novel cages. After having checked the validity of the chosen indices, we sought for less obvious structures and thus screened the cage candidates which ranked slightly above the previously seen architectures. Some examples are presented in figures 4-7, with two, then three types of construction bricks. First the best candidates from $Y_n I_{3/2n}$ families, with the following connecting pattern: Y [a,a,a] and I [-a,-a]



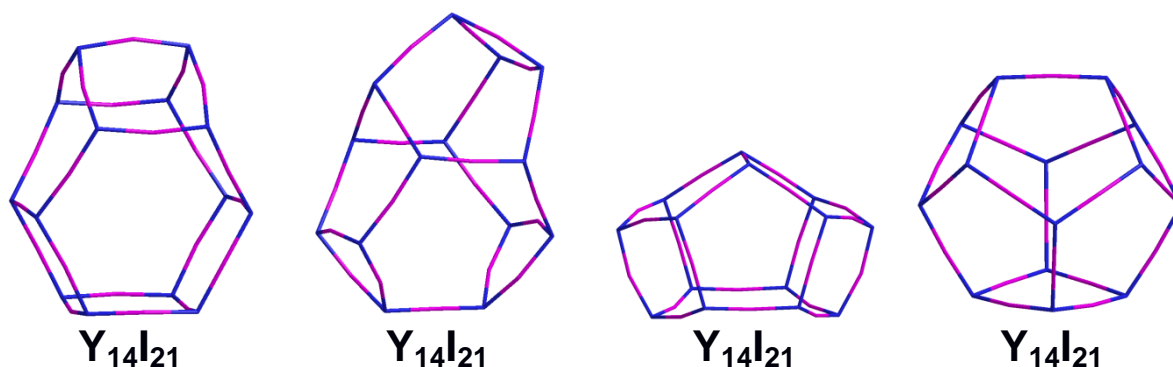


Figure 4. Examples of novel containers discovered in the $Y_n I_{3/2n}$ families.

All of these structures from $Y_n I_{3/2n}$ appear quite symmetrical, although including Y motifs with different environments, there would be not easily conceived “manually”. Conversely such architectures would require properly designed syntheses, since transcription of the modules into real molecular compounds and correct assembly of them into the chosen skeleton is not trivial. This is in strong contrast with the giant assemblies prepared by Fujita, where usually all the modules belong to the same equivalent class. Note that most of the cages in figure 4 possess C_2 symmetry axis, while the three cages on the right column all possess a C_3 symmetry axis, not always easy to catch. We will now examine in more detail the bottom-right one, cage **1** in figure 5.

In $Y_{14}I_{21}$ cage **1**, belonging to the D_{3h} point group, Y modules are present in three different equivalence classes (depicted in blue, yellow and violet colors), so does the I modules (in orange, green and red).

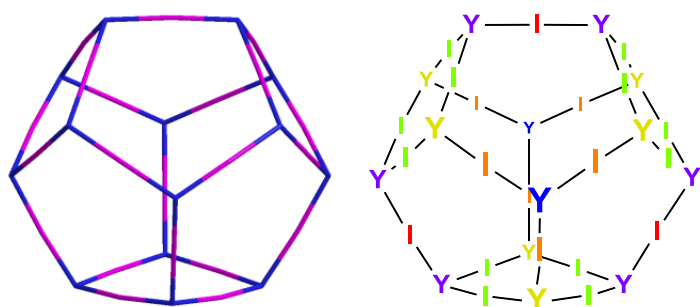


Figure 5. Visualisation of equivalence classes of Y and I chemglyphs in cage **1**.

When now considering cages computed from three types of chemglyphs, even more exotic structures are found. Figures 6 and 7 display examples found in the $X_n V_{2n} I_n$ families, with the following connecting pattern: X [a,a,a,a], V [-a,-a,b] and I [-b,-b].

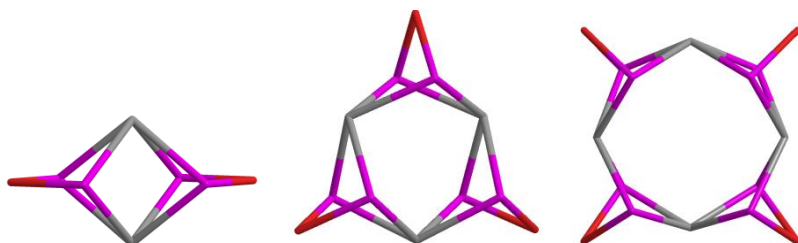




Figure 6. Three crown-like structures from the $X_nV_{2n}I_n$ families.

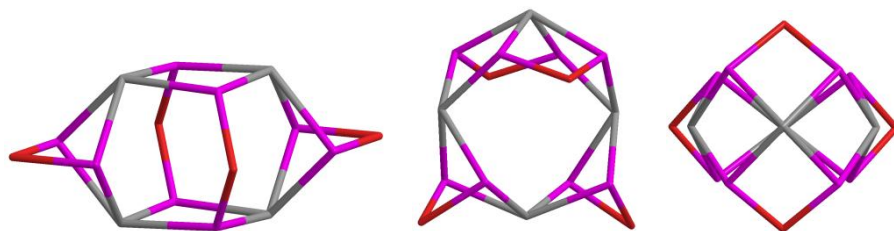


Figure 7. A $X_4V_8I_4$ capsule **2**. (isometric, side, top views).

The next two architectures **3** and **4** in figure 8 are interesting from a structural point-of-view, as being 'diastereomeric' the two couples of 'I' links having the option of being either in an eclipsed (cage **3**) or an alternated (cage **4**) disposition, the central X/V threading being otherwise identical.

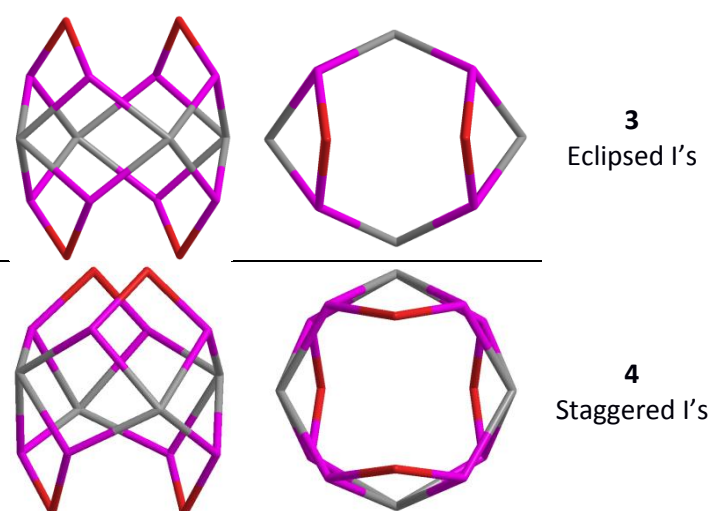
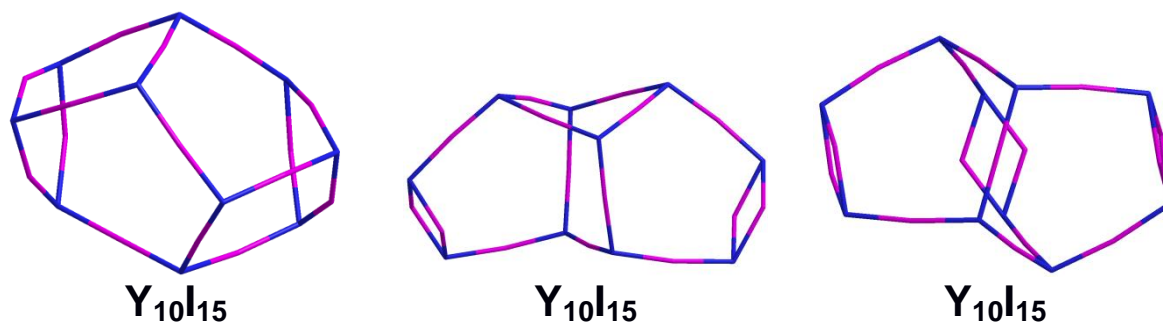


Figure 8. $X_4V_8I_4$ channels with 'diastereomeric' structures **3** and **4** (isometric and top views).

On examination, an even more interesting feature quickly appeared while screening the different libraries: chirality. In several instances two calculated structures were seemingly identical, questioning our protocol of elimination of isomorphic cages. But we recognized that such duplicates were in fact isomeric cages being mirror images, but non-superimposable, hence possessing chirality.

Within the already examined $Y_nI_{3/2n}$ families, varied examples of chiral cages could be spotted and can be seen in figure 9, selected here for possessing a C_2 symmetry axis.



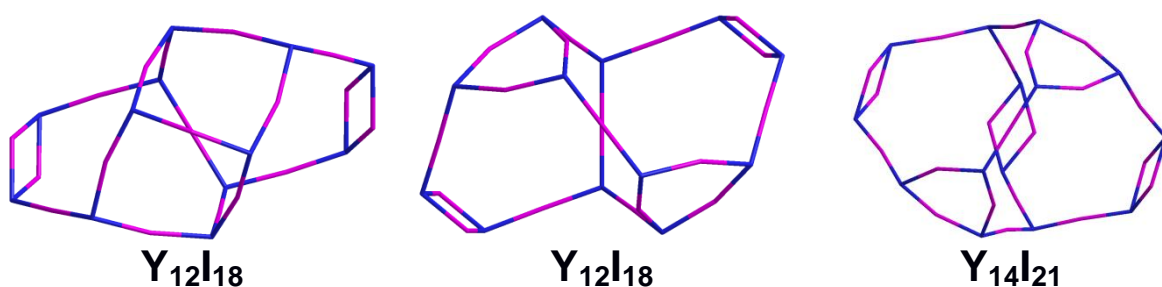


Figure 9. Examples of chiral containers from the $Y_nI_{3/2n}$ families with C_2 symmetry axis.

A nice example of chirality combined with a C_3 symmetry axis was also found with cage **5**:

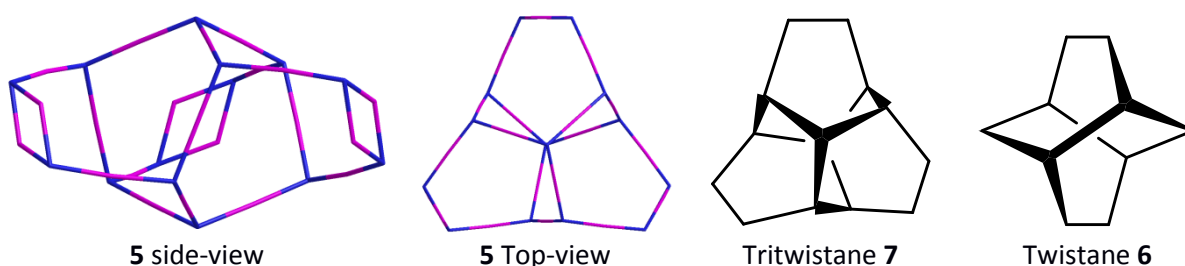


Figure 9. Chiral capsule **5** featuring a C_3 symmetry axis from the $Y_{14}I_{21}$ family, side and top views. Tritwistane **7** and Twistane **6**.

We must stop a moment to define more precisely the chirality at play in these structures.¹⁴ All these architectures, respond to Lord Kelvin's definition of chirality "I call any geometrical figure or group of points chiral, and say it has chirality, if its image in a plane mirror, ideally realized, cannot be brought to coincide with itself."¹⁵ Then as all belong to the class of planar graphs, all can be embedded in a plane without crossing of edges; none would be considered topologically chiral, as would be, for instance, a molecular Moebius band.¹⁶ The proper description is thus 'geometrical chirality' in exactly the same way as for twistane **6**¹⁷ and tritwistane **7**.¹⁸ The latter cage **5** actually closely resembles the Tritwistane **7**. Other examples of intrinsic geometrical chirality can be found in supramolecular entities^{19, 20} in coordination chemistry^{21, 22} metal-organic hybrid cages has been used as chiral containers²³, and enantiomerisation processes of an organic container has been studied.²⁴

The screening of assemblies built from three types of modules gave intriguing chiral architectures, such as the fascinating $X_4V_8I_4$ cage **8**, that can be dubbed 'toy windmill' when considered from an apical point-of-view.

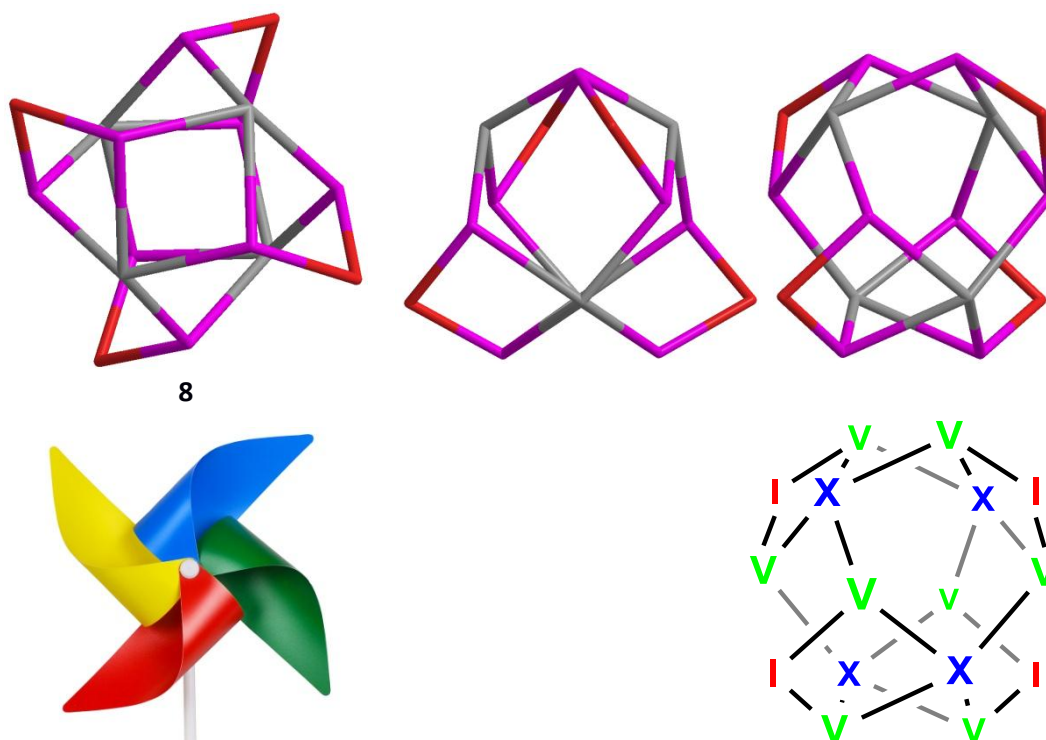


Figure 10. The 'Toy windmill' **8**, a $X_4V_8I_4$ cage; top and two side views. Toy's picture and *chemglyph* representation.

Geometrical oddity went a step further with a group of four $K_2V_4I_6$ cages **9**, **ent-9**, **10** and **ent-10**, that proved to be both chiral and diastereomeric, thus illustrating in topology the famous scholarly example of organic compounds possessing two stereogenic centres forming four isomers, table 5. These "stereogenic centres" would be the two X modules in these structures. Various representations of one molecule of each enantiomeric pairs is drawn in table 6.

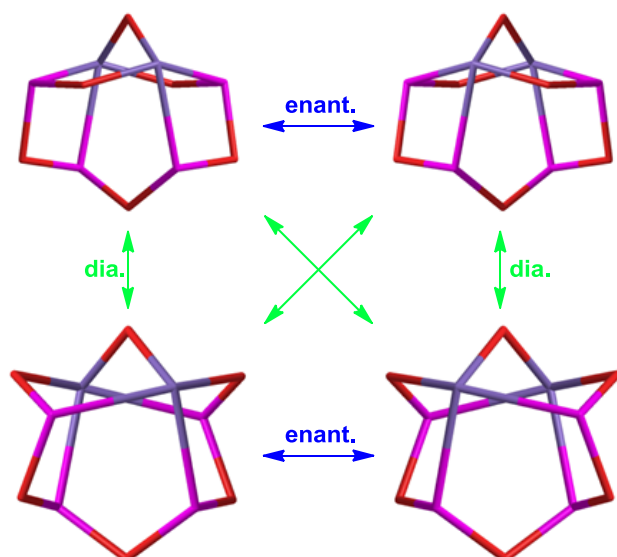


Table 5. Four isomeric cages **9**, **ent-9**, **10** and **ent-10**

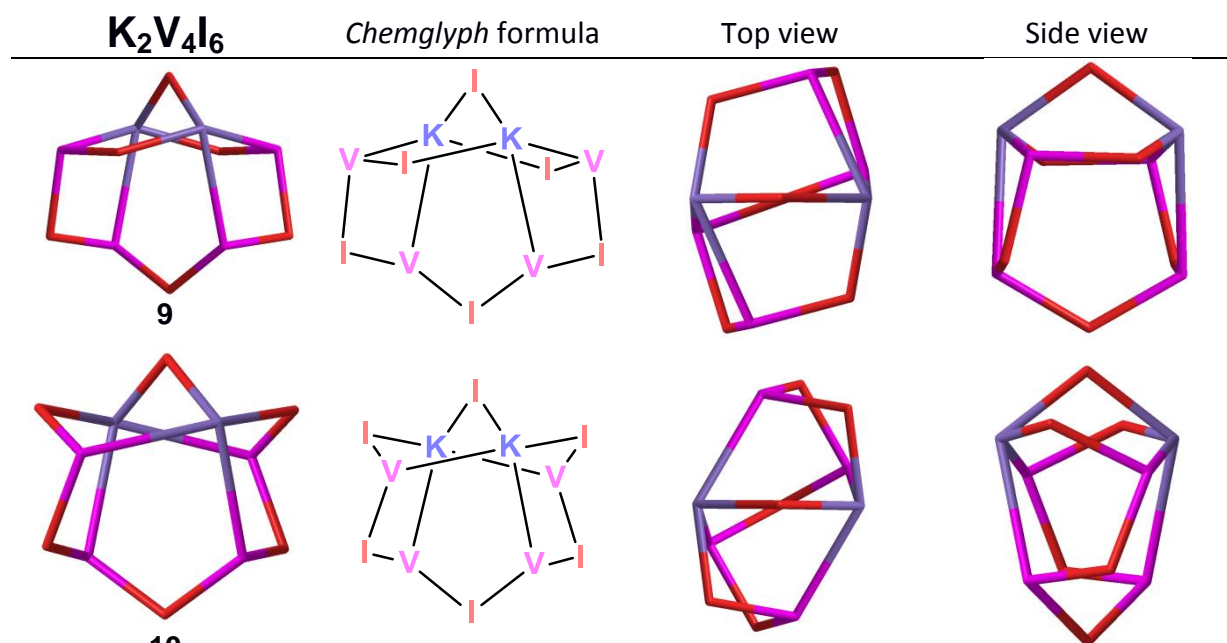


Table 6. Two 'diastereomeric' capsules **9** and **10** both with geometrical chirality, isometric, chemglyph, top and side views.

Now aware of this most important property, we actively searched for chiral cages, seeking specifically for the smallest architecture featuring it. Within the sets that were generated and screened during this project, the structure with a minimal number of elements while chiral was the $Y_2V_3V_3$ cage **11**, with the following connecting pattern $Y[a,a,a] V[-a,b,b] V[-a,-b,-b]$, thus with a total of eight modules, using only two types of bonds (a/-a) and (b/-b).

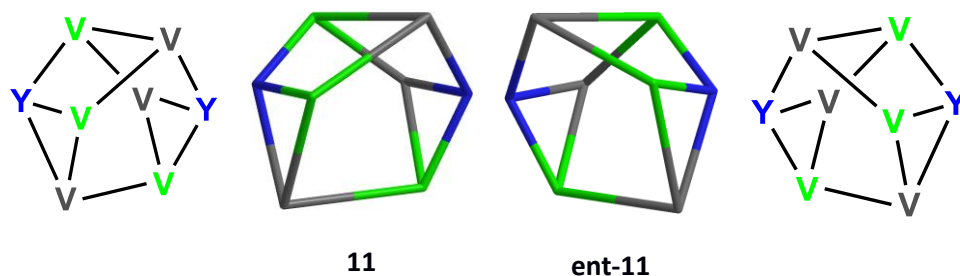
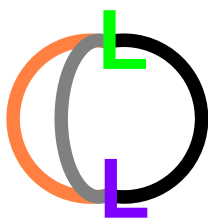


Figure 11. $Y_2V_3V_3$ the smallest topologically chiral container **11** with 2 types of bonds. Chemglyph formula and isometric projection of both enantiomers.

Examining in retrospect the theoretical background at the origin of this chirality, one then sees that the smallest conceivable cage is **12**, a LL' assembly with $L[a,b,c]$ and $L'[-a,-b,-c]$ with a total number of two bricks, however using three different types of bonds (a/-a), (b/-b) and (c/-c).



12

Figure 12. The smallest conceivable chiral cage **12**.

In order to give a more usual depiction of chiral capsules, presented below are molecular transcriptions of two examples, using real atom modules in place of Y and V *chemglyphs*. In the first example with capsule **11**, Y are materialized by a triethanolamine moiety, while V and V' are trisubstituted pyridinic and phenolic fragments.

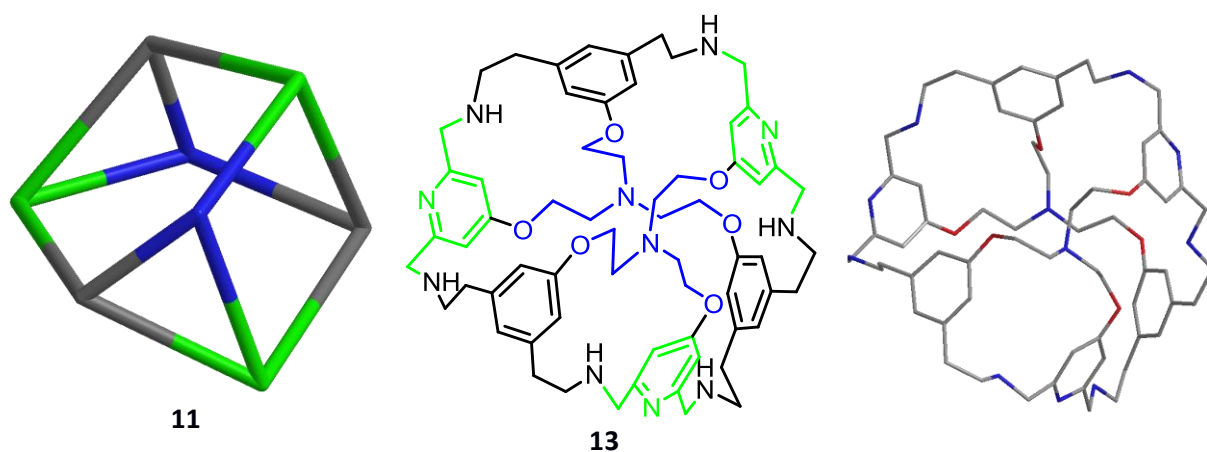


Figure 13. Molecular transcription of chiral cage **11** into cryptand **13**.

The second example with cage **14** comprises a larger total number of modules (25) but using only two *chemglyphs*: Y [a,a,a] and I [-a,-a], with a unique type of bond, (a/-a), and is inferred from a $Y_{10}I_{15}$ architecture. The I *chemglyph* stands for a disubstituted ethane moiety, while the Y is transcribed by nitrogen atoms; hence the whole structure is a particular member of the tren-based azacryptand²⁵ family.

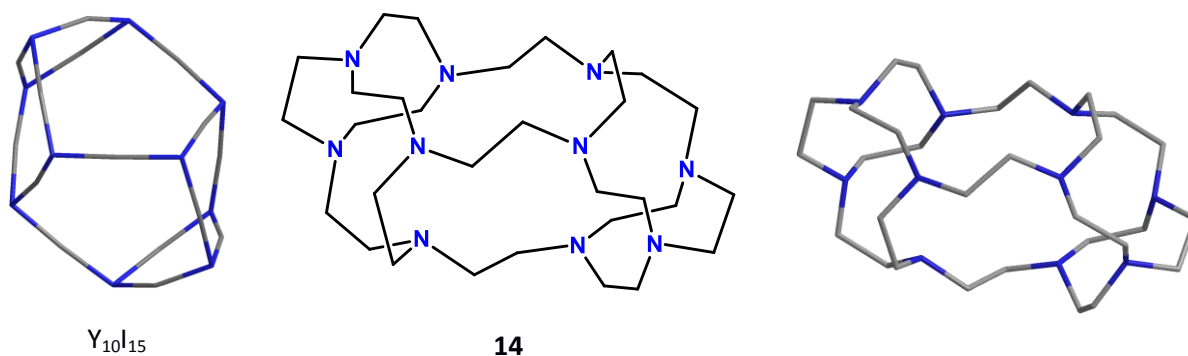


Figure 14. Smallest conceivable azacryptand **14** with geometric chirality.

For an organic chemist it is fascinating to realize that chirality arises simply from the proper combination of ethylenediamine fragments in space, this molecule being, at least virtually, obtainable by simple mixing of ammonia and ethyleneglycol ditosylate. Its official name is 1,4,7,10,13,16,19,22,25,28-decaazahexacyclo[14.14.2.24,10.27,28.213,22.219,25]tetracontane, but the relevant chirality descriptor is still to be defined!

We hope to have convinced the reader of the powerful exploratory potential of *chemglyphs* for the discovery of 3D-architectures with particular structural properties. An optimized generation program was conceived to quickly propose a large variety of containers with levels of complexity relevant to real applications in chemistry. An algorithm based on graph theory allowed us to screen, within the plethora of structures, unique assemblies with structural features complying with chemists needs. The next step, currently under study in our laboratories, is the 'on-demand' conception of containers designed to capture a specific target molecule, or to achieve a particular function, starting from a minimal number of modules with the least synthetic effort needed to prepare it.

¹ Mastalerz, M. Shape-Persistent Organic Cage Compounds by Dynamic Covalent Bond Formation. *Angew. Chem. Int. Ed.* **49**, 5042-5053 (2010).

² Rue, N. M., Sun, J., Warmuth, R. Polyimine Container Molecules and Nanocapsules. *Isr. J. Chem.* **51**, 743 – 768 (2011).

³ Hof, F., Craig, S. L., Nuckolls, C., Rebek, J. Jr. Molecular Encapsulation. *Angew. Chem. Int. Ed.* **41**, 1488-1508 (2002).

⁴ Mastalerz M. Permanent Porous Materials from Discrete Organic Molecules—Towards Ultra-High Surface Areas. *Chem. Eur. J.* **18**, 10082 – 10091 (2012). b) Cooper A. I. Nanoporous Organics Enter the Cage Age. *Angew. Chem. Int. Ed.* **50**, 996 – 998 (2011). c) Holst J. R., Trewin A., Cooper A. I. Porous organic molecules. *Nature Chem.* **2**, 915–920 (2010). d) Tian J., Thallapally P. K.,* McGrail B. P. Porous organic molecular materials. *Cryst. Eng. Comm.* **14**, 1909–1919 (2012).

⁵ a) Bojdy M. J., Briggs M. E., Jones J. T. A., Adams D. J., Chong S. Y., Schmidtman M., Cooper A. I. Supramolecular Engineering of Intrinsic and Extrinsic Porosity in Covalent Organic Cages. *J. Am. Chem. Soc.* **133**, 16566–16571 (2011). b) A Soft Porous Organic Cage Crystal with Complex Gas Sorption Behavior, Mitra T., Wu X., Clowes R., Jones J. T. A., Jelfs K. E., Adams D. J., Trewin A., Bacsa J., Steiner A., Cooper A. I. *Chem. Eur. J.* **17**, 10235 – 10240 (2011). c) Jones J. T. A., Hasell T., Wu X., Bacsa J., Jelfs K. E., Schmidtman M., Chong S. Y., Adams D. J., Trewin A., Schiffman F., Cora F., Slater B., Steiner A., Day G. M., Cooper A. I. Modular and predictable assembly of porous organic molecular crystals. *Nature* **474**, 367–371 (2011). d) Yoon M., Suh K., Kim H., Kim Y., Selvapalam N., Kim K. High and Highly Anisotropic Proton Conductivity in Organic Molecular Porous Materials. *Angew. Chem. Int. Ed.* **50**, 7870–7873 (2011). e) Jin Y., Voss B. A., Noble R. D., Zhang W. A Shape-Persistent Organic Molecular Cage with High Selectivity for the Adsorption of CO₂ over N₂. *Angew. Chem. Int. Ed.* **122**, 6492–6495 (2010).

⁶ a) Breiner B., Nitschke J.R. Reactivity in nanoscale vessels. Chapter in *Supramolecular Chemistry: From Molecules to Nanomaterials*. Gale P.A., Steed J.W. (eds), Wiley, 2011. b) Breiner B., Clegg J. K., Nitschke J. R. Reactivity modulation in container molecules. *Chem. Sci.* **2**, 51–56 (2011).

⁷ Zhang G., Mastalerz M. Organic Cage Compounds - From Shape-Persistency to Function. *Chem. Soc. Rev.* **43**, 1934-1947 (2014).

⁸ a) MacGillivray L. R., Atwood J. L. Spherical molecular containers: from discovery to design. in Gokel G. W. *Advanced Supramolecular Chemistry* Vol. 6, 157-183 (JAI Press Inc. 2000). b) MacGillivray L. R., Atwood J. L. Structural Classification and General Principles for the Design of Spherical Molecular Hosts. *Angew. Chem. Int. Ed.* **38**, 1018-1033 (1999).

⁹ Turner D. R., Pastor A., Alajarin M., Steed J. W. *Molecular Containers: Design Approaches and Applications in Structure and Bonding* Vol. 108, 97–168 (Springer Berlin Heidelberg 2004).

¹⁰ Chakrabarty R., Mukherjee P. S., Stang P. J. Supramolecular Coordination: Self-Assembly of Finite Two- and Three-Dimensional Ensembles *Chem. Rev.* **111**, 6810–6918 (2011).

-
- ¹¹ The Sparsest cut problem is to bipartition the vertices so as to minimize the ratio of the number of edges across the cut divided by the number of vertices in the smaller half of the partition. This objective function favors solutions that are both sparse (few edges crossing the cut) and balanced (close to a bisection).
- ¹² a) Kim K., Ko Y. H., Selvapalam N. *Cucurbiturils: Chemistry, Supramolecular Chemistry and Applications* (Imperial College Press 2014). Reviews: a) Masson E., Ling X., Joseph R., Kyeremeh-Mensaha L., Lua X. Cucurbituril chemistry: a tale of supramolecular success. *RSC Adv.* **2**, 1213-1247 (2012). b) Lee J. W., Samal S., Selvapalam N., Kim H.-J., Kim K. Cucurbituril Homologues and Derivatives: New Opportunities in Supramolecular Chemistry. *Acc. Chem. Res.* **36**, 621-630 (2003).
- ¹³ Liu X., Warmuth R. Solvent Effects in Thermodynamically Controlled Multicomponent Nanocage Syntheses. *J. Am. Chem. Soc.* **128**, 14120-14127 (2006).
- ¹⁴ Mislow K. A Commentary on the Topological Chirality and Achirality of Molecules. *Croatica Chemica Acta* **69**, 485-511 (1996).
- ¹⁵ Kelvin W. T. *Baltimor Lectures on Molecular Dynamics and the Wave Theory of Light.* (C. J. Clay, London 1904) 209-239.
- ¹⁶ a) Walba D. M. Topological stereochemistry. *Tetrahedron* **41**, 3161-3212 (1985). b) Simon J. Topological Chirality of Certain Molecules. *Topology* **25**, 229-235 (1986).
- ¹⁷ Adachi K., Naemura K., Nakazaki M. The Synthesis and the Absolute Configuration of Optically Active [4.4.0.0^{3,8}]Decane. *Tetrahedron Lett.* **52**, 5467-5470 (1968).
- ¹⁸ a) Nakazaki M., Naemura K., Chikamatsu H., Iwasaki M., Hashimoto M. Synthesis and absolute configuration of optically active D₃-tritwistane; the gyrochiral prototype of "twist" diamond. *J. Org. Chem.* **46**, 11, 2300-2306 (1981). b) Nakazaki M., Naemura K., Chikamatsu H., Iwasaki M., Hashimoto M. Synthesis and Absolute Configuration of (-)-D₃-Tritwistane, (-)-(1S,3S,6S,7S,10S,12S)Pentacyclo[8.4.0.0^{2,7}.0^{3,12}.0^{6,11}]Tetradecane. *Chem. Lett.* 1571-1572 (1980).
- ¹⁹ Mateos-Timoneda M. A., Crego-Calama M., Reinhoudt D. N. Supramolecular chirality of self-assembled systems in solution. *Chem. Soc. Rev.* **33**, 363-372 (2004).
- ²⁰ Scarso A., Rebek J. Jr. Chiral Spaces in Supramolecular Assemblies. *Top. Curr. Chem.* **265**, 1-46 (2006).
- ²¹ Seeber G., Tiedemann B. E. F., Raymond K. N. Supramolecular Chirality in Coordination Chemistry. *Top. Curr. Chem.* **265**, 147-183 (2006).
- ²² a) Lehn, J.-M. *Supramolecular Chemistry: Concepts and Perspectives.* (VCH: Weinheim 1995). b) von Zelewsky A. *Stereochemistry of Coordination Compounds.* (John Wiley & Sons Ltd. 1996).
- ²³ a) MacGillivray L. R., Atwood J. L. *Nature* **389**, 469-472 (1997). b) Rivera J. M., Martin T., Rebek J. Jr. *Science* **279**, 1021-1023 (1998). c) Ziegler M., Davis A. V., Johnson D. W., Raymond K. N. *Angew. Chem., Int. Ed.* **42**, 665-668 (2003). d) Seeber G., Tiedemann B. E. F., Raymond K. N. *Top. Curr. Chem.* 265, 147-183 (2006). e) Chapman R. G., Sherman J. C. *J. Am. Chem. Soc.* **121**, 1962-1963, 1999.
- ²⁴ Sun J., Bennett J. L., Emge T. J., Warmuth R. Thermodynamically Controlled Synthesis of a Chiral Tetra-cavitand Nanocapsule and Mechanism of Enantiomerization. *J. Am. Chem. Soc.* **133**, 3268-3271 (2011).
- ²⁵ a) Alibrandi G., Amendola V., Bergamaschi G., Fabbrizzi L., Licchelli M. *Org. Biomol. Chem.* **13**, 3510-3524 (2015). b) Motekaitis R.J., Martell A. E., Dietrich B., Lehn J.-M. *Inorg. Chem* **23**, 1588-1591 (1984). c) Graf E., Lehn J.-M. *J. Am. Chem. Soc.* **97**, 5022-5024 (1975).